IMAGE DOMAIN FEATURE EXTRACTION FROM SYNTHETIC APERTURE IMAGERY

Michael A. Koets and Randolph L. Moses

Department of Electrical Engineering, The Ohio State University
2015 Neil Avenue, Columbus OH 43210, USA

ABSTRACT

We consider the problem of estimating a parametric model that describes radar backscattering from synthetic aperture radar imagery. We adopt a scattering center model that incorporates both frequency and aspect dependence of scattering. We develop an approximate maximum likelihood algorithm for parameter estimation directly on regions of the SAR image. The algorithm autonomously selects model order and structure. Results are presented for both synthetic and measured SAR imagery, and algorithm accuracy is compared with the Cramér-Rao bound.

1. INTRODUCTION

At high frequencies, the scattering response of an object is well approximated as a sum of responses from individual scattering centers [1]. A high-frequency scattering model has been proposed in [2, 3] that incorporates both frequency and aspect dependence of scattering centers. The model is based on dominant responses of monostatic scattering solutions from both Physical Optics and the Geometric Theory of Diffraction. The model generalizes the point scattering model [4, 5], and provides a richer description of scattering behavior. Each scattering center is modeled by a set of parameters describing its location, shape, orientation (pose) and amplitude. These parameters provide a concise, physically relevant description of the object and are thus good candidates for use in target recognition, radar data compression, and scattering phenomenology studies.

The scattering center model is derived as a function of frequency f and aspect ϕ. On the other hand, measurements are typically available in the transform, or image, domain in the form of small image chips extracted from larger SAR images by earlier detection processing stages. To estimate model parameters, these two domains must be bridged in some way.

This work was sponsored by the Defense Advanced Research Projects Agency under contract F33615-97-1020 monitored by Wright Laboratory. The views and conclusions contained in this document are those of the authors and should not be interpreted as representing the official policies, either expressed or implied, of the Defense Advanced Research Projects Agency or the United States Government.

Traditionally, estimation is carried out by transforming image domain data into the frequency domain, and estimating parameters there [5, 6]; however, this requires estimation of high order models must be applied to large data sets. Alternatively, Gerry *et. al.* [3] transforms the model into the image domain. Unfortunately, the transformation is analytically intractable unless simplifying assumptions are made that limit the applicability of the approach.

We present a novel hybrid approach that provides good statistical properties at low computational cost. Our approach is to estimate parameters in the image domain while retaining a frequency domain scattering model. We exploit the localized scattering and noise correlation behavior to decompose the problem into smaller estimation problems of lower model order on subregions of the image. The algorithm operates directly on SAR image chips and fit models only on regions of high backscattered energy. Processing on image chips facilitates insertion into SAR ATR data processing streams. In addition, by model fitting only on regions of the image we realize robustness to the assumed clutter model; for example, we reduce uncertainty or bias in feature estimates that might be caused by large nearby clutter scattering that is not well modeled as Gaussian noise. We also obtain about two orders of magnitude of computational speedup over the algorithm in [3] under a less restrictive class of SAR measurement geometries and image formation algorithms.

2. PARAMETER ESTIMATION PROBLEM

We adopt the scattering model developed in [2, 3]. The backscattered energy of an object can be modeled as a sum of contributions of individual scattering centers modeled as:

$$m(f,\phi;\theta) = \sum_{i=1}^{K} m_i(f,\phi;\theta_i) \tag{1}$$

where $\theta^T = [\theta_1^T, \ldots, \theta_K^T]$ and

$$\begin{aligned} m_i(f,\phi;\theta_i) &= A_i \cdot \left(j\frac{f}{f_c}\right)^{\alpha_i} \\ &\quad \cdot \exp\left(\frac{-j4\pi f}{c}(x_i\cos\phi + y_i\sin\phi)\right) \end{aligned}$$

$$\cdot \operatorname{sinc}\left(\frac{2\pi f}{c} L_i \sin(\phi - \overline{\phi_i})\right)$$
$$\cdot \exp(-2\pi f \gamma_i \sin\phi) \quad (2)$$

This model describes the responses of both localized scattering centers, such as trihedrals, and distributed scattering centers such as dihedrals. Here, f is frequency, ϕ is aspect angle, f_c is the center frequency, and c is the propagation velocity. Each $m_i(f, \phi; \theta_i)$ is the predicted scattering center response described by the parameter vector $\theta_i = [A_i, x_i, y_i, \alpha_i, L_i, \overline{\phi}_i, \gamma_i]^T$; A_i is a complex-valued amplitude, x_i and y_i are the downrange and crossrange locations, $\alpha_i \in [-1, -1/2, 0, 1/2, 1]$ describes its frequency dependence, L_i and $\overline{\phi_i}$ are the length and tilt angle of a distributed scattering center, and γ_i models the (mild) aspect dependence of a localized scattering center. For a localized scattering center, $L_i = \overline{\phi_i} = 0$, and for a distributed scattering center $\gamma_i = 0$.

SAR data measurements are taken on a $M_f \times M_\phi$ grid of (f, ϕ) values; we model the measurements as a sum of a model term and Gaussian noise. Stacking the measurements into an $M \times 1$ vector $\tilde{d}$, with $M = M_f M_\phi$, we have

$$\tilde{d} = \sum_{i=1}^{k} \tilde{m}_i + \tilde{n} \quad (3)$$

where $\tilde{n} \sim \mathcal{N}(0, \tilde{\Sigma})$ and each $\tilde{m}_i$ is a vector of $m_i(f, \phi; \theta_i)$ samples on the measurement grid. Image formation is accomplished by interpolating to a rectangular grid, multiplying with a 2D window function, zero padding, and transforming with a 2D inverse discrete Fourier transform. We arrive at a grid of $N_x \times N_y$ samples in the image domain, where $N = N_x N_y > M$ because of the zero padding. The image formation process can be represented by a linear operator B. Stacking the image-domain measurements into an $N \times 1$ vector d, we have

$$d = B\tilde{d} = \sum_{i=1}^{k} m_i + n \quad (4)$$

where $n \sim \mathcal{N}(0, \Sigma)$ and $\Sigma = B\tilde{\Sigma}B^H$.

3. ML ESTIMATION AND APPROXIMATION

From the model and measurement vector above, we can state the estimation problem as follows: given $d \in \mathcal{R}(B)$, find the maximum likelihood estimate of θ. From equation (4), we see that $d \sim \mathcal{N}(m(\theta), \Sigma)$. Since $d \in \mathcal{R}(B)$, the θ which minimizes the log likelihood function is found as:

$$\hat{\theta}_{ML} = \arg\min_{\theta} J(\theta) \quad (5)$$

$$J(\theta) = [d - m(\theta)^H]\Sigma^\dagger[d - m(\theta)] \quad (6)$$

where $(\cdot)^\dagger$ denotes Moore-Penrose pseudoinverse. Equation (5) is a nonlinear least squares minimization problem; because d and θ are of high dimension, direct minimization is computationally intensive, and we seek computationally simpler suboptimal solutions.

We make use of the fact that scattering center responses are localized in the image domain. Therefore, for parameter vectors near the ML estimate the above minimization can be approximately decomposed into smaller estimation problems. We partition the image into r regions R_i of high energy and a remainder region R_0. Defining Π_i as the projection onto region R_i, we have

$$J(\theta) = \sum_{i=0}^{r} [d - m(\theta)^H]\Pi_i\Sigma^\dagger\Pi_i[d - m(\theta)]$$
$$\approx \sum_{i=1}^{r} [d - m(\theta^i)]^H\Pi_i\Sigma^\dagger\Pi_i[d - m(\theta^i)] + C \quad (7)$$

where $\theta^i = [\theta_{i_1}^T, \ldots, \theta_{i_{l(i)}}^T]^T$ is a vector containing the scattering parameters for region R_i and C is a constant independent of θ. Since the number of pixels in R_i is (much) less than N and the θ^i form a disjoint partition of θ, the individual minimization problems in equation (7) are decoupled and of (much) smaller size.

An additional advantage of the approximate ML algorithm is its robustness to the assumed noise model. The assumption of correlated Gaussian noise across the entire image is not very accurate for scenes where clutter is present in the form of trees, power lines, etc. However, this assumption is much better over small image regions that primarily contain target scattering centers.

4. ALGORITHM DESCRIPTION

The parameter estimation algorithm uses equation (7) with an estimate-and-subtract approach similar to the CLEAN algorithm [7]. We recursively locate the highest energy region, fit a small number of scattering centers to that region, and subtract the reconstructed model from the original data. This models the region of interest and also removes sidelobes from the remainder of the image. If sidelobe leakage into other regions is not a problem, the regions can be processed in parallel rather than recursively. The algorithm terminates when a specified number of scattering centers have been processed, when a specified fraction of energy in the original image has been modeled, or when the peak in the residual data is a specified level below the original peak.

We segment the high energy regions using a watershed-based algorithm [8]. We classify the image region as a distributed scattering center, a single localized scattering center, or multiple localized scattering centers using moments of inertia of the image region about a vertical and a horizontal axis through the center of mass of the region.

We compute initial estimates for the parameter values from the measured data in the image region or assign initial values based on knowledge of the range of values that are reasonable to represent the scattering mechanisms. We choose x and y as the center of mass of the region. We estimate L by computing an DFT of a one dimensional slice of the image data through the center of mass of the selected image region, removing the window function, and fitting a quadratic function to the peak of the main lobe of the sinc; L is found from the quadratic coefficients. The α parameter is drawn from a small set of discrete values and an exhaustive search is possible. We set $\gamma = \overline{\phi} = 0$, and initialize A by a linear least squares fit over the region. Once initial parameters are set, we use a standard nonlinear minimization routine to descend to a local minimum.

We have implemented a fast version of the estimation algorithm which employs a slight variation of the initialization step and skips the iterative descent [9]. This version requires two orders of magnitude less computation, but produces less accurate results.

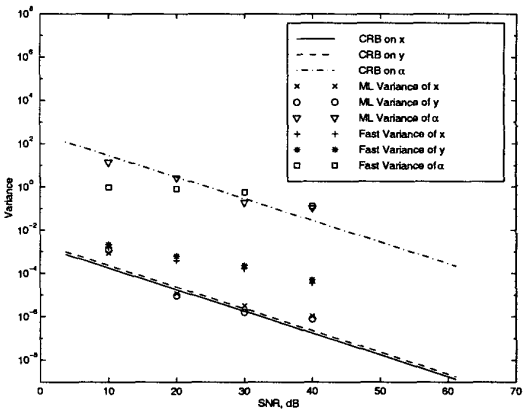

Figure 1: Observed parameter variances Cramér-Rao Bounds for XpatchF SLICY trihedral at 6" Resolution.

5. EXPERIMENTAL RESULTS

We present feature extraction experimental results on three data sets: 1) synthesized model data, 2) XpatchF synthesized data of a Sandia National Laboratory test target (SLICY), and 3) measurements of a T72 tank.

To test the relative statistical efficiency of the approximate maximum likelihood method, we synthesized noisy images of localized and distributed scattering centers at several SAR image resolutions using the parametric model. We performed 50 such trials for each combination of scattering center type, resolution, and signal to noise ratio. The AML parameter estimator essentially achieves the Cramér-Rao bound (CRB) in every case [9].

We next applied our algorithms to synthetic images of the SLICY geometric test object that were generated using the XPatchF electromagnetic prediction package. The frequency and aspect responses were generated by XPatchF, and different ranges of frequencies and aspects were used to form images with different resolutions. We added noise to the synthetic images and estimated the scattering center parameters with both the fast and the approximate ML variations of the algorithm. We compared simulation variances with Cramér-Rao bounds for a number of scattering centers on the object for several SAR image resolutions and SNRs. We present two examples for the trihedral scatterer. The observed variances and the CRB for the x, y, and α parameters of the scattering center for 6" resolution imagery and for several SNR values is shown in Figure 1. Here, SNR is defined as the ratio of the peak pixel in the noiseless data to the standard deviation of the noise. The observed variances of the parameter estimates and the CRB are shown in Figure 2 for 3", 6", and 12" SAR resolutions and at 30 dB SNR. Variances for x and y parameters are in inches^2 for these figures. In both cases we see good agreement with the CRB for the AML algorithm, and somewhat higher variances for the fast estimation algorithm; however, even in the fast algorithm the standard deviations of scattering center locations are less than 0.1 inch for all noise levels and resolutions.

We have also applied our algorithms to measured SAR images [10]. Figure 3 shows a measured SAR image of a T-72 tank and its reconstruction from parameter estimates. We estimated the parameters of 33 scattering centers in this image. The algorithm autonomously selects model order and modeling regions. The algorithm models 71% of the overall image energy, and 85% of the energy in a rectangular region containing the target. In addition, the tank barrel segment is modeled as a single scattering center whose length is modeled within 10 cm of the 1.37 m length. In comparison, peak-based scattering center extraction methods model this segment as multiple peaks spread along the barrel. This suggests that the proposed model can be used to extract geometric scattering information such as length, and that it can be accurately estimated on measured data.

6. CONCLUSIONS

We have developed a computationally efficient algorithm for estimating scattering parameters from SAR image chips. The algorithm recursively estimates small clusters of scattering centers from regions of high energy in the SAR image, providing both computational efficiency and robustness to the assumed noise model. The algorithm autonomously selects model order and structure. Simulations on synthetic

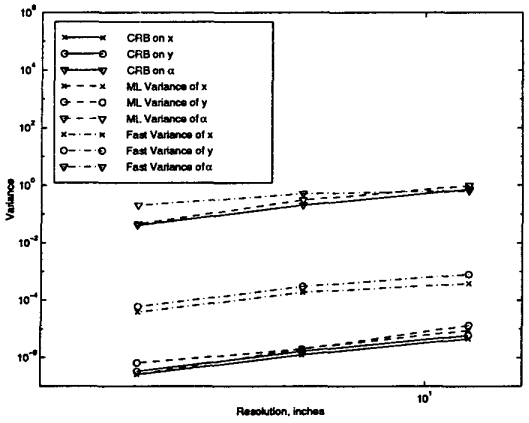

Figure 2: Observed parameter variances and Cramér-Rao Bounds for Xpatch SLICY trihedral at 30 dB SNR and 3", 6", and 12" resolutions.

and measured imagery suggest that the algorithm is nearly statistically efficient, and shows promise for extracting physically meaningful scattering features.

7. REFERENCES

[1] J. B. Keller, "Geometrical theory of diffraction," *J. Opt. Soc. Am.*, vol. 52, no. 2, pp. 116–130, 1962.

[2] M. Gerry, *Two-dimensional inverse scattering based on the GTD model.* PhD thesis, The Ohio State University, Columbus, OH, 1997.

[3] M. J. Gerry, L. C. Potter, I. J. Gupta, and A. van der Merwe, "A parametric model for synthetic aperture radar measurements," *IEEE Transactions on Antennas and Propagation.* submitted, April 1997.

[4] M.-W. Tu, I. Gupta, and E. Walton, "Application of maximum likelihood estimation to radar imaging," *IEEE Transactions on Antennas and Propagation*, vol. 45, no. 1, pp. 20–27, 1997.

[5] J. J. Sacchini, W. M. Steedly, and R. L. Moses, "Two-dimensional Prony modeling and parameter estimation," *IEEE Transactions on Signal Processing*, vol. 41, pp. 3127–3137, November 1993.

[6] L. C. Potter and R. L. Moses, "Attributed scattering centers for SAR ATR," *IEEE Transactions on Image Processing*, vol. 6, pp. 79–91, January 1997.

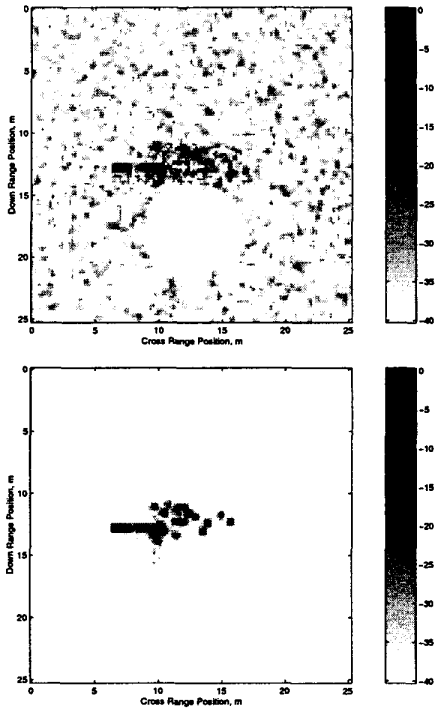

Figure 3: Measured SAR Image of T-72 Tank (top) and reconstruction from estimated parameters (bottom). Images are in dB magnitude

[7] J. Tsao and B. D. Steinberg, "Reduction of sidelobe and speckle artifacts in microwave imaging: The CLEAN technique," *IEEE Trans. Ant. Prop.*, vol. 36, pp. 543–556, April 1988.

[8] J. Stach and E. LeBaron, "Enhanced image editing by peak region segmentation," in *Proceedings of the 1996 AMTA Symposium*, October 1996.

[9] M. Koets, "Automated algorithms for extraction of physically relevant features from synthetic aperture radar imagery," Master's thesis, The Ohio State University, Columbus, OH, 1998.

[10] *MSTAR (Public) Targets: T-72, BMP-2, BTR-70, SLICY.* Available at http://www.mbvlab.wpafb.af.mil/public/MBVDATA.